40th Fluid Dynamics Conference and Exhibit
28 June - 1 July 2010, Chicago, Illinois

AIAA 2010-4728

Design of a Glass Supersonic Wind Tunnel Experiment for Mixed Compression Inlet Investigations

Daniel S. Galbraith[1], Mark G. Turner[2], Paul D. Orkwis[3] and Marshall C. Galbraith[4]
University of Cincinnati, Cincinnati, Ohio, 45221

and

James F. Driscoll[5] and Ethan Eagle[6]
University of Michigan, Ann Arbor, Michigan, 48128

Mixed compression inlets offer a great increase in pressure recovery compared to conventional external compression inlets at Mach numbers above two. These inlets suffer from problems with shock wave boundary layer interactions (SBLI) which cause flow instabilities and severe performance reductions. Previous experiments conducted at the University of Michigan used a wind tunnel with glass side walls with an extensive test section to measure the SBLI associated with a single oblique shock. This work presents a redesign of the single oblique shock experimental setup, using computational fluid dynamics, to also include a downstream normal shock with a diffuser. The new experimental configuration will provide insights into the effects that combined oblique/normal shock boundary layer interactions have on the health of the boundary layer in the diffuser section of a mixed compression inlet. The extensive glass walls of the wind tunnel will allow direct access for optical measurements of the shock boundary layer interactions and the diffuser section.

Nomenclature

AIP	=	Aerodynamic Interface Plane
CFD	=	Computational Fluid Dynamics
NSH	=	Normal Shock Holder
k	=	Turbulent Kinetic Energy
M	=	Mach number
M_∞	=	Inflow Mach number
OSG	=	Oblique Shock Generator
SBLI	=	Shock wave boundary layer interaction
UM	=	University of Michigan
UC	=	University of Cincinnati
ε	=	Eddy dissipation
ω	=	Specific dissipation rate

I. Introduction

Mixed compression inlets provide a greater total pressure recovery than standard external compression inlets for flight Mach numbers above two. These inlets operate by creating a shock train that travels down the diffuser followed by a normal shock, as seen in Figure 1. Inviscid theory shows that static pressure increases with little total pressure loss due to the combination of oblique shocks and a weaker terminal normal shock. However, for

[1] MS Graduate Student, Department of Aerospace Engineering & Engineering Mechanics, 745 Baldwin Hall ML 0070, PO Box 210070, Cincinnati, OH 45221-0070, AIAA Student Member.
[2] Associate Professor of Aerospace Engineering & Engineering Mechanics, Department of Aerospace Engineering & Engineering Mechanics, AIAA Associate Fellow.
[3] Professor of Aerospace Engineering & Engineering Mechanics, Department of Aerospace Engineering & Engineering Mechanics, AIAA Associate Fellow.
[4] PhD Graduate Student, Department of Aerospace Engineering & Engineering Mechanics, AIAA Student Member.
[5] Professor, Aerospace Engineering Department, AIAA Fellow.
[6] Doctoral Candidate, Aerospace Engineering Department, AIAA Student Member.

viscous flows these inlets experience SBLIs leading to boundary layer separation and increased total pressure loss that can prevent the inlet from starting. The adverse effects of the SBLIs can be reduced by bleeding out the separated region using aspiration. Sub boundary layer micro ramps have also been used which produce a pair of vortices that effectively cut through the separation bubble, reducing its size. Previous experiments have been conducted to study a single oblique shock reflection by Babinsky[1], Doerffer, et al.[2], and Lapsa[3]. This work is meant as a continuation by following the oblique reflection with a normal shock and a subsonic diffuser, in order to more closely resemble a realistic inlet configuration. This new configuration is being designed via a collaboration between the University of Michigan (UM) and the University of Cincinnati (UC). Wind tunnel experiments are being conducted at UM, while UC is conducting Computational Fluid Dynamics (CFD) simulations on the proposed geometries. The new experiment is being designed with relatively simple geometry to simplify CFD simulations, so that it can be used as a CFD validation test case.

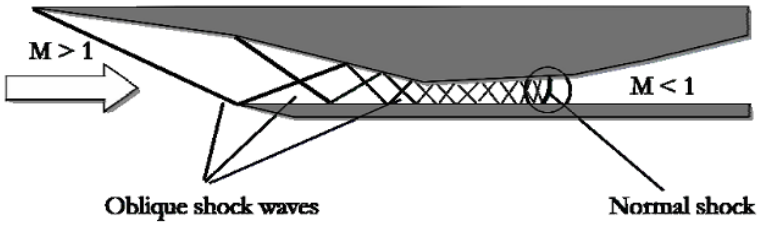

Figure 1. Shock train in a mixed compression inlet.[4]

II. Previous Experiments

Previous experiments custom built at UM to investigate oblique SBLIs were performed at a Mach number of 2.75 in a vacuum driven tunnel. The test section was 36in long and with a 2.25x2.75in cross section with glass side walls. A SBLI was created by inserting a 7.75° wedge onto the top wall of the wind tunnel to serve as an oblique shock generator (OSG), as shown in Figure 2. The OSG was placed at the far downstream end of the tunnel where the boundary layers would be the thickest in order to increase the resolution of the stereo particle image velocimetry (SPIV) measurements of the boundary layers. However, in this configuration the tunnel did not start. After several design iterations the configuration shown in Figure 3 was found that allowed the tunnel to start. The final configuration consisted of an OSG that was located half the length of the test section downstream of the throat. In addition, the OSG was lowered from the top wall in order for the leading edge to see the supersonic core flow, and not the sub sonic boundary layer. Most importantly, the span of the OSG was reduced from the full span of 2.25in to a span of 1.25in in order to reduce tunnel blockage. Three OSG angles were made: 7.75°, 10° and 12°.

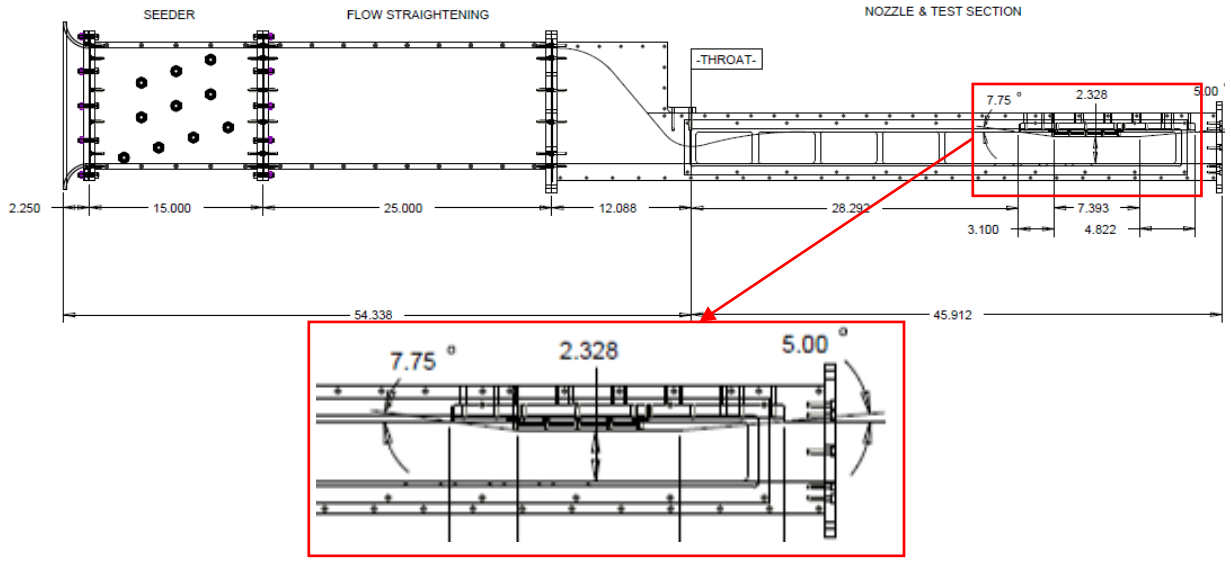

Figure 2. Wind tunnel schematic with the initial OSG installed in the aft segment of the test section.

This configuration was provided as a blind test case to be analyzed using CFD. A workshop was held in Orlando in January 2010 to present the results. An overview of the CFD comparisons is presented by DeBonis et al[5]. One of the current authors analyzed this configuration, but those results could not be submitted since he had access to the experimental results. Some of these results are shown for the M 2.75, 7.75° OSG. Figure 4 shows the computed center plane Mach number for the configuration in Figure 3, and shows a clean SBLI. While this region is ideal, the outside of the side plates produces large vortical separations, as seen in Figure 5. These structures did not prevent the wind tunnel from starting, but required much time and effort to effectively resolve with CFD. Inadequate resolution of these vortical structures can prevent the CFD solution from converging to a steady state, making their existence less desirable in a CFD validation experiment.

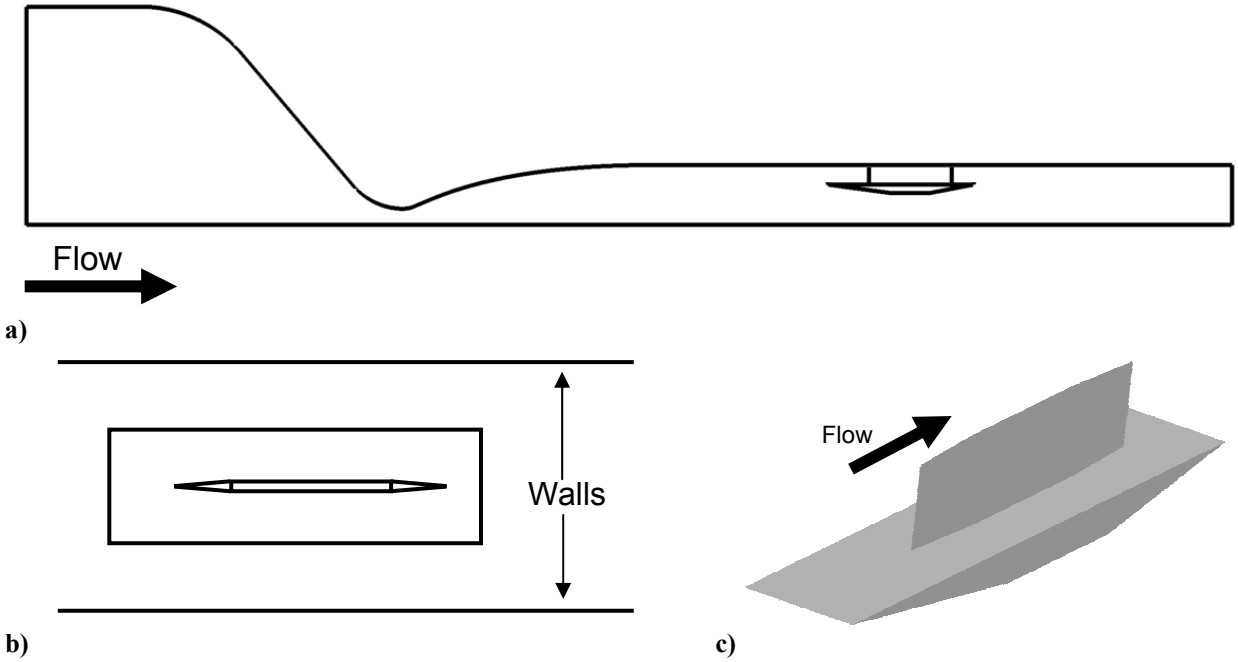

Figure 3. Half span OSG used for previous SBLI experimental study and CFD validation. a) Side view of the tunnel and OSG. b) Top view of OSG relative to the tunnel walls. c) Isometric view of the OSG.

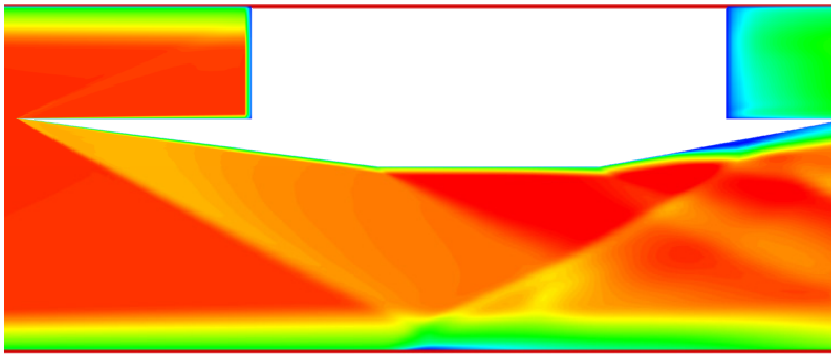

Figure 4. Center plane Mach number (0-2.75) for the 7.75° OSG.

Figure 6 shows iso-surfaces of density gradients in the streamwise direction colored by the derivative of the density gradients in the streamwise direction. This figure shows many shocks, including the desired oblique shock and reflection, but also the shocks emanating from the center strut leading and trailing edge, along with a vortex along the side of the OSG. The leading and trailing edge shocks from the vertical support spill over the sides of the OSG and into the region underneath the OSG.

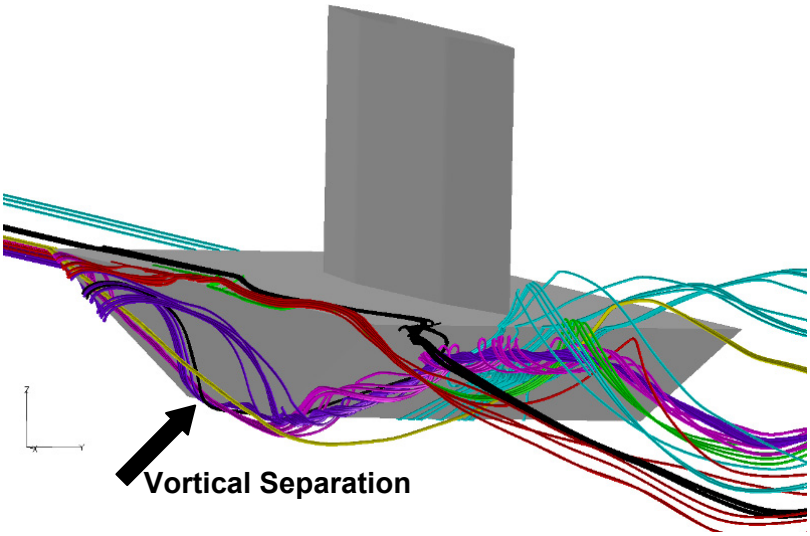

Figure 5. Vortical separation off the side of the OSG.

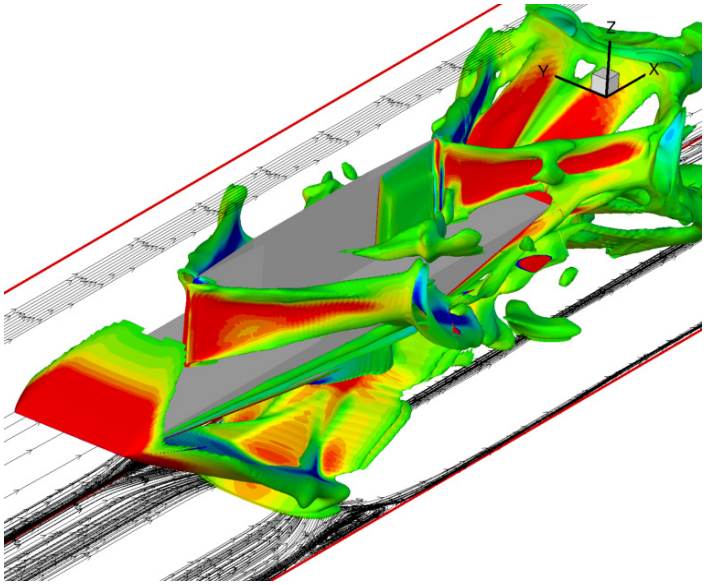

a)

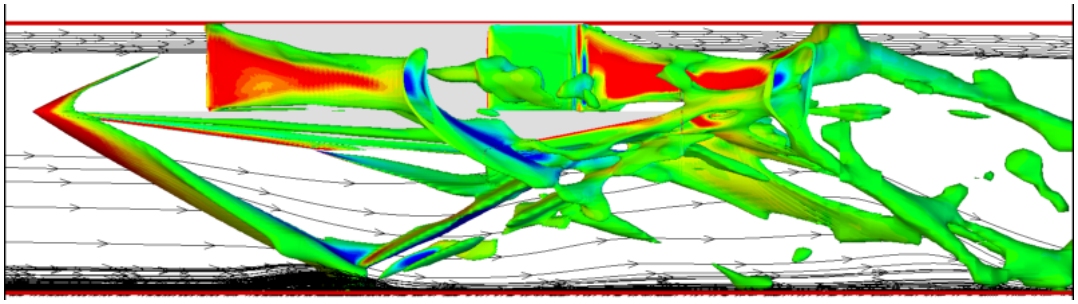

b)

Figure 6. Iso-surfaces of density gradients in the streamwise direction, colored by the derivative of the density gradients in the streamwise direction. a) Isometric view. b) Side view.

In this work a full span OSG is proposed to remove the interaction between the regions above and below the OSG and approach more a realistic inlet geometry. This has the added benefit of replacing the single vertical support in the center of the tunnel with two side supports immersed in the side wall boundary layers which reduces the flow field blockage.

III. Design Procedure

The primary purpose of this study is to investigate the effects of an oblique shock reflection followed by a normal shock and a subsonic diffuser on the boundary layer of a mixed compression style inlet. Since the region of interest is the lower wall, the top wall can be configured to generate the required shocks without resembling a realistic inlet geometry. Using these ideas, a full-span OSG is placed in the test section to create the oblique and reflected shocks. A normal shock holder (NSH) is placed downstream of the OSG at a location where the reflected shock will pass between the OSG and NSH. This will transmit the reflected shock to the region above the NSH, and results in the desired main flow field containing one oblique shock reflection followed by a normal shock. The NSH also aids in the positioning of the normal shock; making its location less sensitive to the back pressure since the space between the OSG and NSH acts as an automatic relief valve. The basic design is arrived at by considering two-dimensional inviscid theory coupled with some basic SBLI principles. Three-dimensional viscous effects are not considered in the preliminary design phase; viscous effects are later considered by analyzing the preliminary design using CFD.

The goal of the experiment is to mimic the final oblique and normal shocks in a mixed compression inlet. To achieve this, an experimental design that satisfies the following criteria was sought:

1) The bottom wall boundary layer should experience an oblique shock reflection followed by a normal shock.
2) The pressure rise across the oblique shock reflection should be approximately 2.
3) The distance between the oblique shock reflection and the normal shock should be approximately 15 undisturbed boundary layer thicknesses.
4) The incident Mach number to the normal shock should be less than 1.3.
5) The normal shock should occur at the beginning of a subsonic diffuser.
6) The Mach number downstream of the diffuser should be approximately 0.55.
7) The boundary layer incoming to the oblique SBLI should be fully turbulent and at least 0.25in high.

Based on measurements from Settles and Lu[6], a pressure rise across the incident and reflected shock of two would result in a SBLI for the oblique shock reflection with at most a minor separation bubble. A minor separation bubble is desirable for the initial configuration to limit the possibility of the following normal shock creating a massive separation bubble. A larger oblique SBLI separation bubble can later be induced by increasing the angle of the OSG. In addition, by separating the oblique shock reflection 15 boundary layer thicknesses from the normal shock, the boundary layer has some time to recover from the shock reflection before being hit by the normal shock. The separation distance is expected to further help in limiting the separation at the normal shock, as well as prevent the two separation bubbles merging into a single separation bubble. An incident Mach number of 1.3 in front of the normal shock is chosen to mimic the final normal shock strength expected in a mixed compression inlet. After the normal shock, the flow will be diffused to Mach 0.55 to represent conditions at the aerodynamic interface plane (AIP) to an engine. A fully turbulent boundary layer approximates the real inlet boundary layer, and the boundary layer height ensures adequate field of view for the SPIV technique[7].

It is important to note that the initial design process relies solely on inviscid theory. A shock train calculator coded in MATLAB[8] determines the shock generator ramp angle based on the inlet Mach number, and the desired Mach number in front of the normal shock using an iterative scheme. This calculator was also used to create Figure 7, which contains three curves describing the Mach number in front of the normal shock based on the OSG angle and the inflow Mach number (M_∞). Based on inviscid theory, an inflow Mach number of 1.80 and OSG ramp angle of 7.17^o are required to achieve the desired normal shock incident Mach number and pressure rise across the oblique SBLI of roughly two. The leading edge of the shock generator is placed 1.5 boundary layer thicknesses from the top wall to allow the leading edge to be located in the core flow while maximizing the mass flow under the OSG. Exposing the leading edge to core flow produces the inviscid shock angle as well as prevents the separation bubble that would form if the leading edge of the OSG was mounted to the ceiling of the wind tunnel. In order to allow the normal shock to be placed 15 boundary layer heights from the oblique shock reflection, the tunnel height needs to be doubled from the existing 2.75in test section to a proposed 5.5in. The boundary layer thickness used for preliminary two-dimensional CFD calculations was estimated from a three-dimensional Mach 2.00 calculation of the existing wind tunnel without an OSG or NSH. Based on the initial two-dimensional CFD calculations, the viscous oblique shock reflection was approximated by an inviscid shock reflection that reflects two boundary layer thicknesses

above the tunnel floor, due to the presence of the boundary layer. The ramp extends from the leading edge of the OSG to within two boundary layer thicknesses of the oblique shock reflection, as shown in Figure 8.

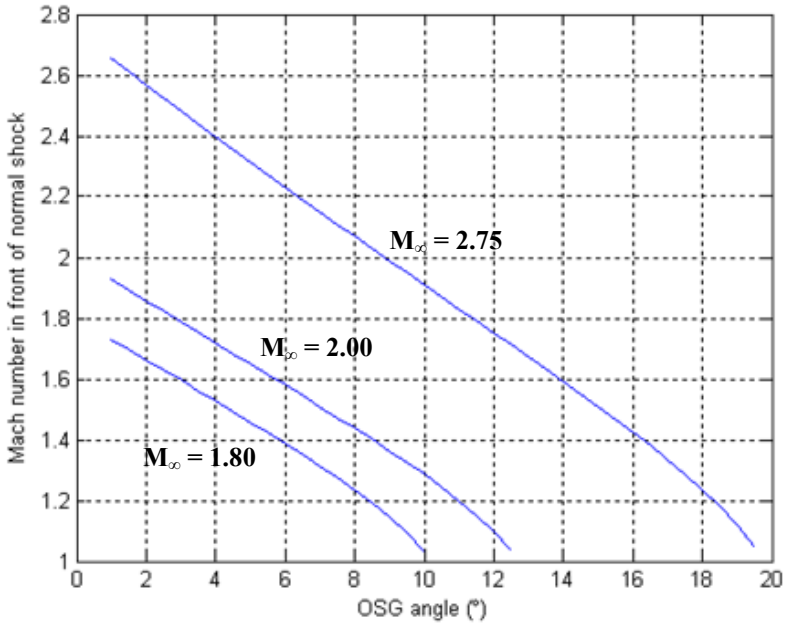

Figure 7. Normal shock Mach number for varying OSG ramp angle based on the inflow Mach number.

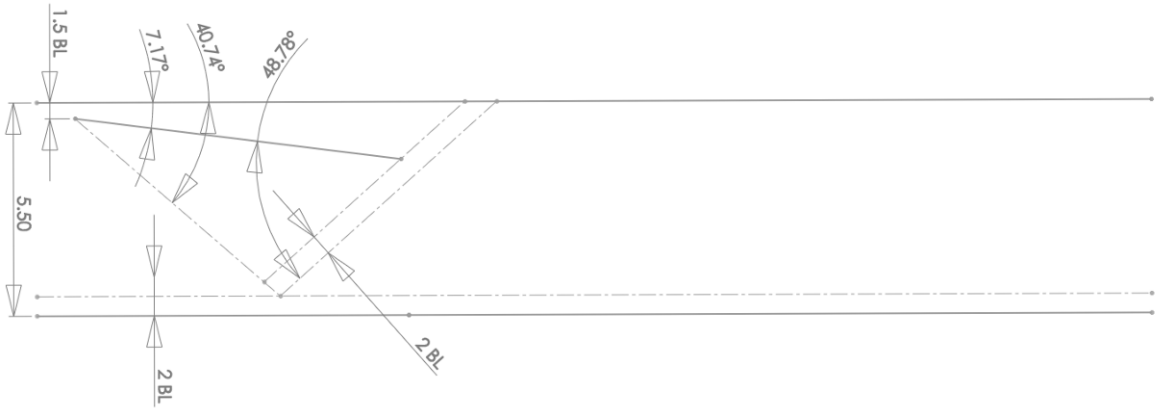

Figure 8. OSG and calculated oblique incident and reflected shocks.

The NSH is located so that the leading edge coincides with a line parallel to the reflected shock, but offset downstream by two boundary layer thicknesses. A wedge angle of 10° on the upper surface of the NHS was set, and the NSH was then designed to taper down in the downstream direction in order to alleviate start up problems that may occur due to a constant area duct, as shown in Figure 9.

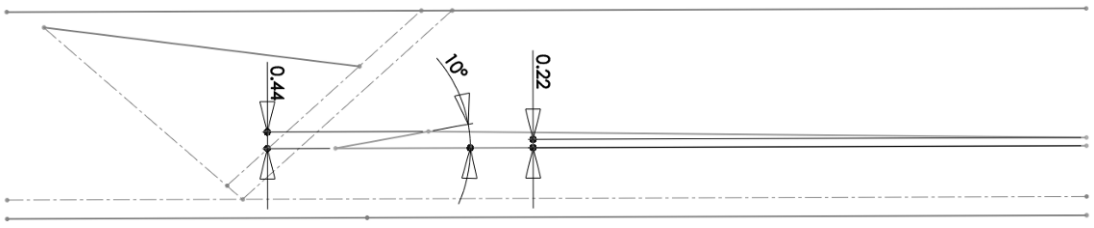

Figure 9. Addition of NSH.

The Mach angle at the lower trailing edge of the OSG determines the maximum vertical location of the shock holder. The Mach cone intersects the NSH 0.1in downstream of its leading edge, as shown in Figure 10 and the close up in Figure 11. This allows for the largest area possible under the NSH while maintaining the two boundary layer thickness safety factor for the reflected shock and ensuring that the resulting expansion wave at the lower corner of the OSG does not interact with the normal shock below the NSH.

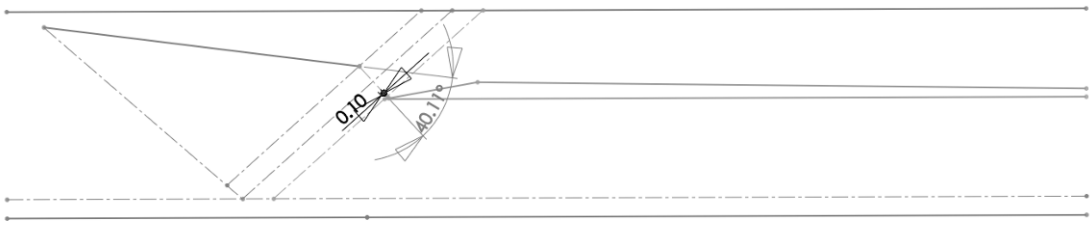

Figure 10. Criteria for the placement of the NSH.

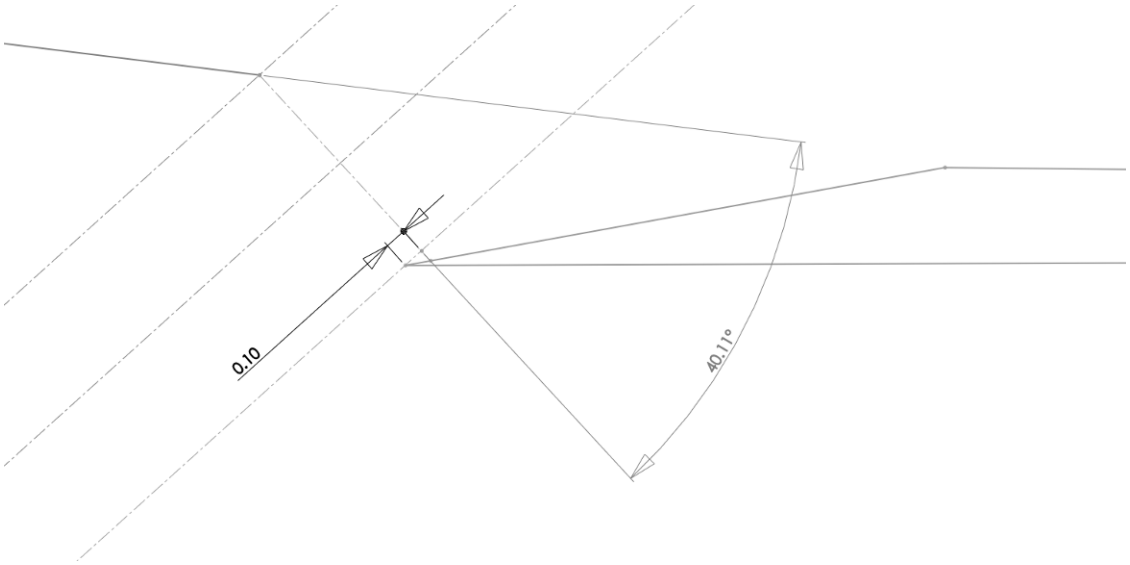

Figure 11. Close up of the leading edge placement of the NSH relative to the Mach cone.

Knowing the geometry of the NSH, the OSG can be completed by making its top wall slope downward at 2° and the back wall expand 5° relative to the NSH, as shown in Figure 12. A slanted upper surface of the OSG accounts for boundary layer growth and reduces the likelihood of choking. However, a large slope results in a strong supersonic expansion which subsequently shocks down at the trailing edge of the OSG to equalize pressure. This in turn creates a separation bubble on the ceiling of the tunnel just downstream of the trailing edge of the OSG. While this separation bubble is not of concern for the experiment, it causes additional difficulties for a CFD calculation since its size must be accurately computed. Hence, the slope on the upper surface of the OSG was set to 2° to limit flow expansion and the subsequent tunnel ceiling separation bubble. The slope on the back wall was also chosen to ensure an expansion in the channel formed between the OSG and NSH, thus preventing the channel from choking.

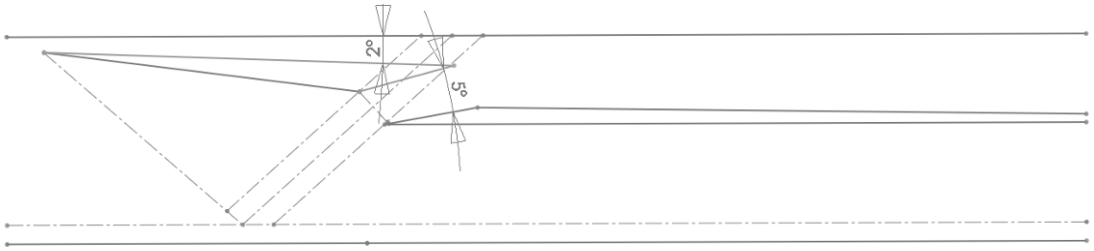

Figure 12. Completed OSG.

The beginning of the diffuser is located 7/8 the distance between the oblique shock reflection and the leading edge of the NSH in order to reduce the effects on the normal shock of the expansion wave at this corner. The diffuser floor slopes downward at 4° to diffuse the flow to Mach 0.55. The required area ratio for the diffuser is based on the Mach number at the leading edge of the NSH and the desired exit Mach number of 0.55. This configuration is shown in Figure 13 and the completed design in Figure 14.

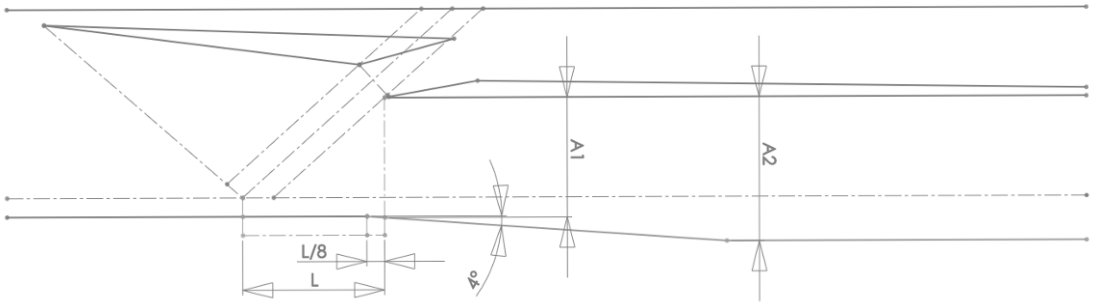

Figure 13. Addition of a diffuser section.

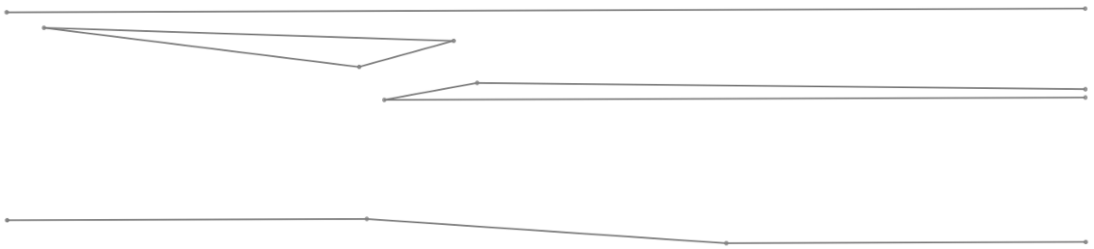

Figure 14. Completed 2D profile of the OSG and NSH with a diffuser in the wind tunnel.

The design is extruded for three-dimensional CFD calculations to create a model with the OSG and NSH spanning the full tunnel width. The design of the test section is a fully parametric model that is dependant on the inlet Mach number and shock generator ramp angle only. The sidewalls are glass, which cannot support the OSG or NSH. They must be supported from above, and this will be done with supports at the sides. The overall area must also account for this additional blockage.

IV. Flow Solver

All CFD solutions are obtained with the OVERFLOW[9] flow solver which utilizes the Chimera overset mesh technique[10]. The Navier-Stokes equations are solved using a third order accurate upwind finite volume scheme using the HLLC[11] model combined with the Koren[12] limiter. The time integration uses an unfactored SSOR implicit solution algorithm[13] and multi-grid is utilized to accelerate convergence to a steady state. Further convergence gains are achieved by initializing computations of the entire wind tunnel via inviscid 1D nozzle theory. This produces an initial solution with subsonic flow upstream of the throat that accelerates through the throat and then remains at a constant supersonic Mach number through the entire test section.

V. Mesh and Boundary conditions

An overset mesh topology technique was chosen to ease the meshing procedure. While the geometry is relatively simple, the overset mesh technique allows the mesh point density in a certain region to be altered without having to modify the remaining domain. Pointwise[14] and a package of in-house software at the UC Gas Turbine Simulation Laboratory (GTSL) were used for the mesh generation. The 2D mesh in Figure 15 has 382 thousand points in 13 blocks and y+ values less than 2 everywhere, except at the leading edge of the NSH where it is less than 4. The 3D mesh in Figure 16 has 8.5 million points in 14 blocks and y+ values less than 1.

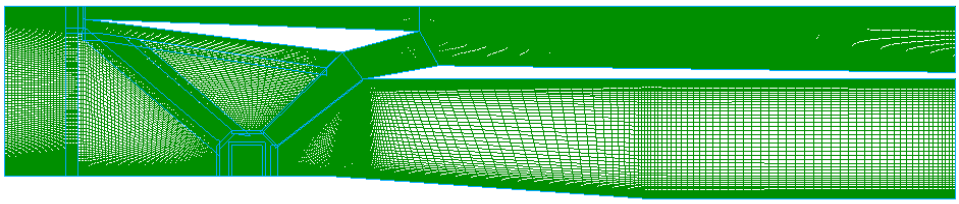

Figure 15. 2D mesh for Mach 1.80 case with OSG and NSH.

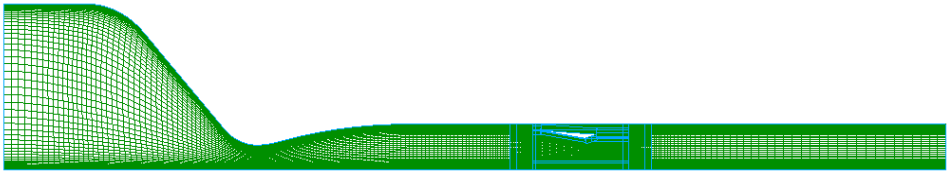

a)

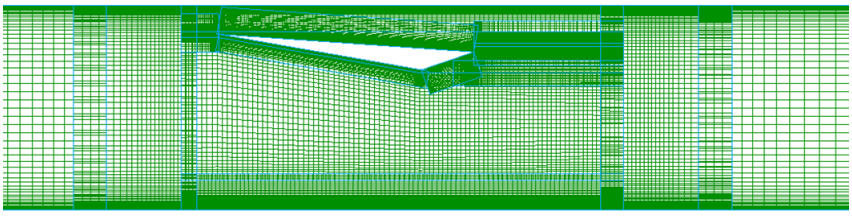

b)

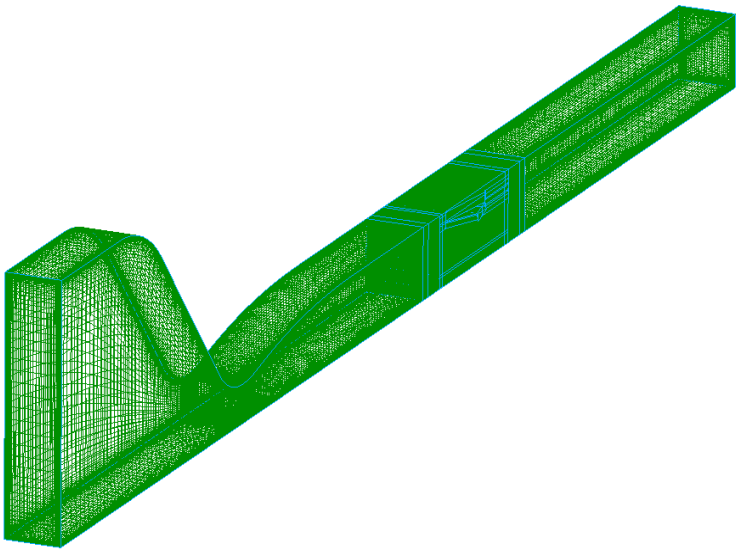

c)

Figure 16. 3D mesh for Mach 2.00 nozzle with 10° OSG configuration. a) Side view. b) Close up of the test section. c) Iso view of the mesh.

Overflow is highly parallel, and the blocks can be decomposed in such a way as to create a parallel simulation that is balanced. Typical runs use 20-90 cores and take 2-8 hours. Care must be taken to fully converge a solution to make sure it is truly steady. A solution can appear to be unchanging, although slowly growing separation regions can cause the oblique shock to move upstream and out the inlet, possibly preventing the tunnel from starting. These corner region separations grow slowly because of the small local time steps associated with constant CFL values for steady state solvers. While the transients are not temporally accurate they do offer clues to tunnel start dynamics.

In all cases a nozzle inlet boundary condition is used which extrapolates mass flow based on the total temperature and total pressure. A pressure outflow boundary condition is used at the tunnel exit, and all solid walls are modeled with viscous, adiabatic walls using pressure extrapolation.

VI. Results

This section presents first a summary of two-dimensional results obtained for the idealized preliminary geometry. Presented next is a study of possible configurations that could utilize existing inlet geometry. These configurations are assessed using steady state simulations to determine if the tunnel will run if started. The results for several possible modifications that run are then presented. Preliminary experience is then reported for time accurate simulations that start with quiescent flow.

A. Two Dimensional Preliminary Design Simulations (Mach 1.80, 5.50in Height, 10° OSG)

The initial two-dimensional CFD results are summarized in Figures 17 and 18, which show computed Mach number and density gradient contours respectively for the 5.5in tall configuration. The inlet boundary condition was generated from a constant area duct, since an actual Mach 1.80 nozzle geometry does not currently exist for the experimental facility. This duct is computed in isolation and then a slice of the solution is taken from the point where the boundary layers correspond to the desired thickness. This slice is then used as the inlet boundary condition.

As shown in the figures, the initial configuration has a diffuser starting half way between the oblique shock reflection and the NSH leading edge. The simulations show a large separation bubble at the beginning of the diffuser that creates a shock wave at the diffuser entrance. To reduce the effect of this shock, the beginning of the diffuser was moved back to 7/8 the distance between the oblique shock and shock holder leading edge. This was the first of several design changes driven by the CFD findings.

Figure 17 also shows the flow acceleration in the channel above the OSG and the shock system that equalizes the pressure aft of the OSG. Although the upper channel is not generally considered important for a SBLI study it does become important if it chokes or unstarts. The CFD results show a shock system that induces a large separation on the ceiling. This system must be considered because it limits the effective expansion of the upper channel flow and could prevent tunnel start.

The two dimensional preliminary design simulations demonstrate that the desired design parameters can be obtained with the proposed configurations. However, they do not include three-dimensional effects, which will be shown to be extremely important.

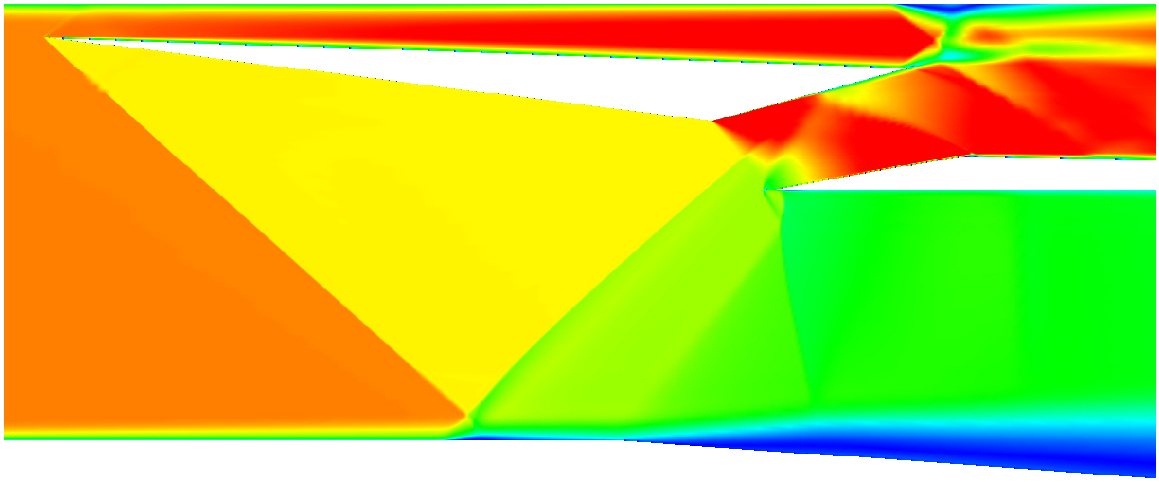

Figure 17. 2D results for the 5.50in tunnel with Mach 1.80 inflow. Contours of Mach number ranging from Mach 0-2.

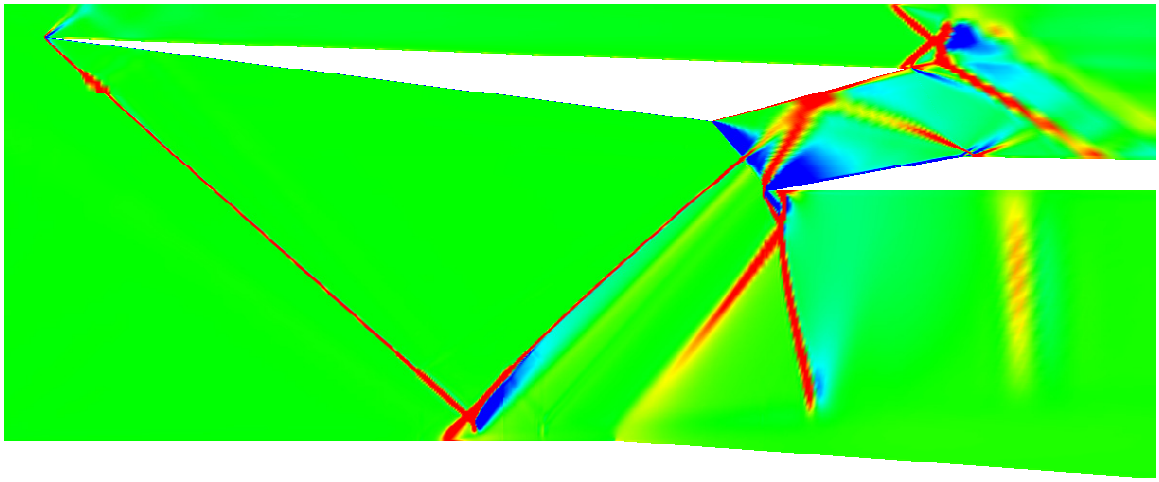

Figure 18. 2D results showing contours of density gradients. Red areas represent shocks while blue areas represent expansions.

B. Modified Configuration Studies Aimed at Existing Tunnel Geometry

It should be noted that the two dimensional design discussed above requires the construction of a new wind tunnel inlet, hence, the team decided to explore whether a design could be created that would utilize one of the existing wind tunnel inlets for Mach numbers 2.00 or 2.75. The authors noted that the previous investigations with this tunnel had difficulty starting if the shock generators spanned the entire tunnel, and that this led to a partial span OSG design in the previous work that produced very three dimensional flow. To explore these possibilities and understand better the starting problem, experiments were performed sans a NSH to investigate the flow field generated by a single OSG in the current 2.25x2.75in test section tunnel at Mach numbers of 2.00 and 2.75.

With this in mind, Table 1 illustrates the 3D CFD simulations completed to identify the running limitations of the tunnel, initially with only the OSG installed. This table shows the parameters that were modified in order to explore the sensitivity of the design: tunnel geometry, design Mach number, wedge angle, wedge length, and tunnel width.

Table 1. Configurations simulated to investigate running limitations.

Design Mach Number	Width (in)	Length (% of initial design)	OSG Angle (°)	Tunnel Start?
2.75	4.50	100	10.0	Yes

2.75	2.25	100	10.0	Yes
2.00	4.50	100	10.0	No
2.00 (Inverted nozzle)	2.25	100	10.0	No
2.00	2.25	100	10.0	No
2.00	2.25	75	10.0	No
2.00	2.25	50	10.0	Yes
2.00	2.25	75	8.5	No
2.00	2.25	50	8.5	Yes

C. Turbulence Model

Experiments showed that the Mach 2.75 cases with a 10° wedge angle would start. However, the initial CFD simulations predicted corner separation growth in the tunnel which prevented the passage under the OSG from starting. These simulations were obtained with a 3rd order accurate representation of the SST turbulence model. The turbulence model was reduced to 1st order accuracy while maintaining a 3rd order accurate discretization of the Navier Stokes equations. This resulted in the simulated tunnel starting and matching the experimental experience. It was found that the higher order turbulence model produces overshoots and undershoots of k, ω and ε that caused the separation bubbles to grow and prevent the simulated tunnel from starting. The 1st order SST model has more dissipation and allowed the tunnel to start; hence it was used for all future calculations. It is recognized that the SST model may produce larger separations and blockage than reality, but since the CFD is being used to design the experiment, a conservative approach was taken.

D. Mach 2.00 Cases

The preliminary design was based on a Mach 1.80 flow, hence it was felt that the closest existing nozzle would be the Mach 2.00 configuration. Unfortunately, it was found that this geometry was even harder to start numerically than the Mach 2.75 case, even with the 1st order SST model. The initial Mach 2.00 configuration was computed with a 10° OSG but would not start. Detailed analysis of the solution found that the flow coming out of the supersonic nozzle was top/bottom asymmetric, with thicker boundary layers on the bottom wall. The nozzle was inverted so as to place some of the OSG metal blockage in the fluid blockage, since there were greater losses already on the lower wall, with the thought of possibly reducing the overall blockage. Unfortunately, this effect was not great enough to allow the tunnel to start and the inverted nozzle concept was abandoned.

Wedge length and angle were the next parameters to be investigated. The length of the OSG was reduced in order to reduce the blockage in the tunnel. A more benign 8.5° OSG was also tested, which produced a Mach number of 1.4 in front of the NSH, just above the desired 1.3 Mach number. The OSG length was reduced to 75% and 50% of its original length. Unfortunately, neither 75% case started for the 10° or 8.5° OSG angles, but both cases started with the 50% length wedge, indicating that the reduction in blockage was sufficient. However, the 50% length option is undesirable because it results in significant flow field nonuniformity entering the diffuser. In addition, the NSH would need to be positioned within the flow boundary layer in order for the expansion fan from the lower trailing edge of the OSG to impinge on the upper surface of the NSH. However, the results do suggest further study is warranted directed at finding a combination of length and angle that might be more beneficial.

It should be noted that these simulations are steady state and do not simulate the start up of the tunnel in a physically realistic unsteady manner. However, they do indicate whether a certain configuration runs if started. The authors realize that this is a less restrictive condition and is not sufficient to demonstrate actual starting but is a necessary condition. The design process assumes that once a starting configuration is found with steady state analysis, unsteady simulations can be conducted to explore the unsteady startup transients.

E. Started Tunnel Configuration Results

The next sections present the cases from Table 1 that started.

1. Effect of Higher Mach Number (Mach 2.75, 2.25x2.75in, 10° OSG)

A 10° full span OSG experimental configuration developed to study starting criteria is being used in experimental tests with the Mach 2.75 nozzle at UM, and was also simulated at UC. The CFD results in Figure 19 show the Mach 2.75, 2.25in tall tunnel. The boundary layers seem thicker than in the 5.50in tall tunnel, but this is due to the height difference of the tunnel. Furthermore, this simulation is computed with an actual nozzle, rather than a manufactured inlet condition, hence producing more accurate boundary layers. An oblique shock can be seen generated off the OSG that reflects off the tunnel floor. This creates a small bubble of low velocity flow in the

bottom wall boundary layer. This low velocity region then generates a compression wave upstream of the shock reflection. It can also be seen that the bottom corners of the tunnel generate large separated flow regions. These are the features that can easily grow until the passage below the OSG chokes, and prevents the tunnel from starting. The turbulence intensity is also shown in each of these solutions since the turbulence model has considerable influence on the separated regions, and hence the overall solution. The turbulence intensity calculated is very low (less than 0.2%) in the free stream, but is much larger in the boundary layers as expected.

Also shown in the figure is a three dimensional plot of the flow field containing isosurfaces of a small value of negative streamwise velocity to identify the separated flow regions. These plots should be compared for each configuration as they give a qualitative view of the corner separations that govern this flow field.

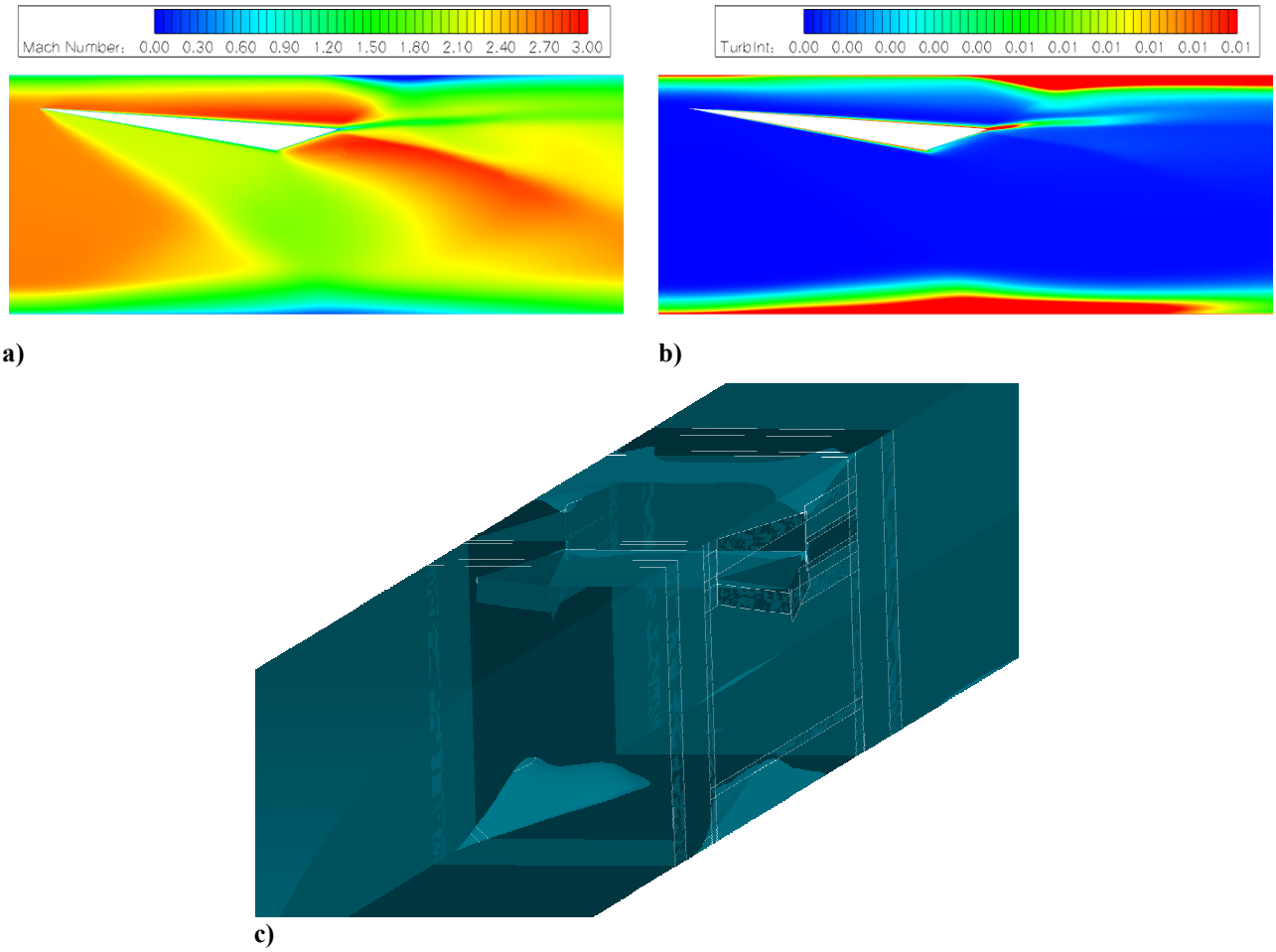

Figure 19. Mach 2.75, 10° OSG case. a) Tunnel centerline colored by Mach contours from 0.0 – 3.0, b) Tunnel centerline colored by turbulent intensity contours from 0 – 1% c) Tunnel with iso surfaces of separated regions.

2. Effect of Tunnel Width (Mach 2.75, 4.50x2.75in, 10° OSG, double wide)

It was felt that the corner separation blockage could be reduced if the tunnel were twice its original width, i.e., broadened from 2.25in to 4.50in. A mesh was generated for this configuration with double the number of spanwise points, hence maintaining the same grid quality as the 2.25in wide case. The solution obtained with the double width tunnel is shown in Figure 20. A very similar flow field was produced, with the exception of a small separation bubble on the floor of the tunnel towards the centerline. The absolute blockage however is very similar to the 2.25in width case, showing that absolute blockage is relatively independent of the tunnel width but its three dimensional distribution might change. It is good to note that the SBLI looks much cleaner; resembling a 2D SBLI with a more defined reflected shock of the leading edge of the separation bubble in this configuration compared to the 2.25in

wide tunnel. However, it is again noted that this configuration produces a higher post reflected shock Mach number than desired.

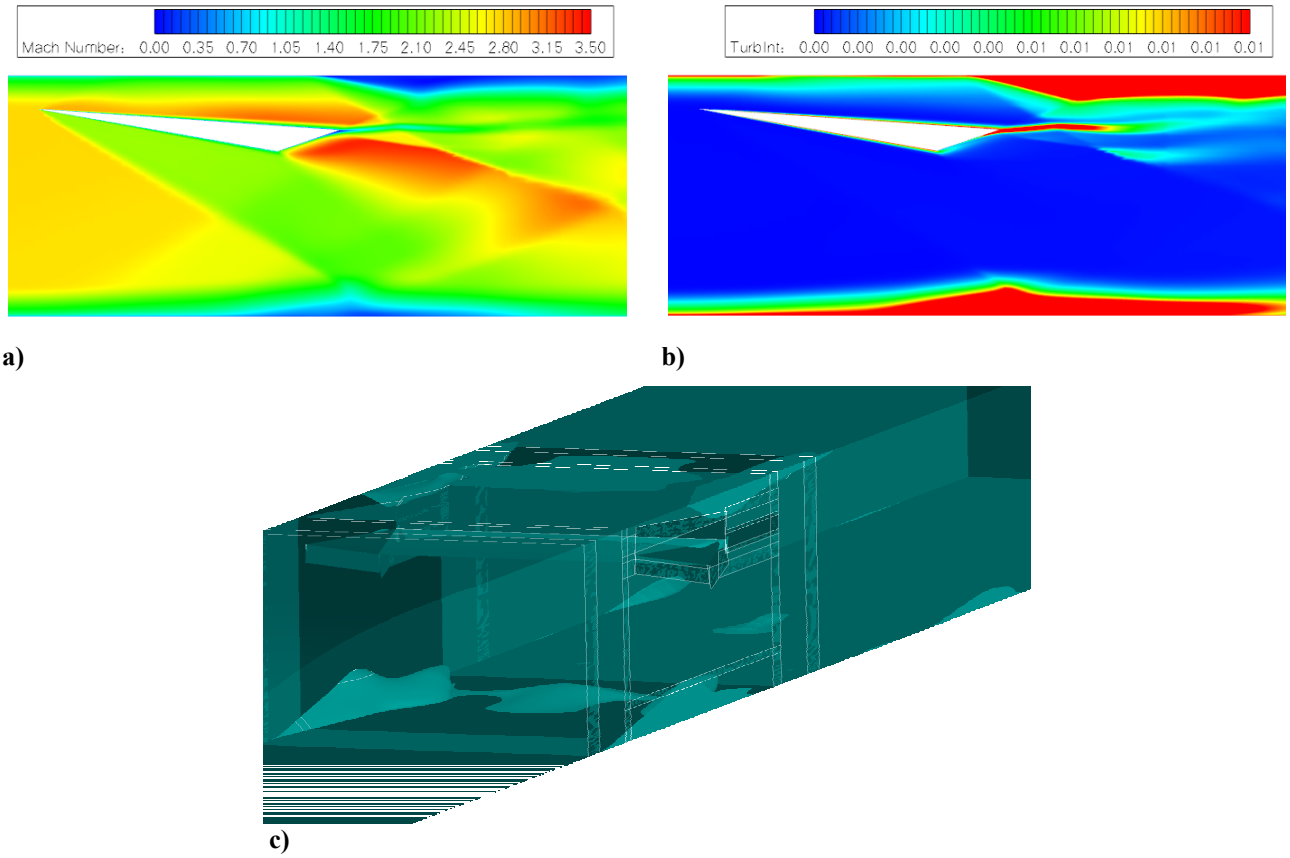

Figure 20. Mach 2.75, 10° OSG case. a) Tunnel centerline colored by Mach contours from 0.0 – 3.0, b) Tunnel centerline colored by turbulent intensity contours from 0 – 1% c) Tunnel with iso surfaces of separated regions.

3. Effect of Mach number and Wedge Length (Mach 2.00, 2.25x2.75in, 10° OSG, 50% wedge design length)

The 10° wedge case was computed with the Mach 2.00 nozzle. The tunnel failed to start in this, due to the large corner separations along the bottom wall growing until the channel below the OSG choked. The OSG was scaled down to 75% of its design length, which reduced its thickness and the blockage in the tunnel. This configuration also failed to start for the same reasons. The OSG was then shortened to 50% of the design length, and this configuration allowed the tunnel to start, as shown in Figure 21. However, an installed NSH in this configuration would have very nonuniform flow before the normal shock and as such does not meet the design requirements. In order to intersect the expansion wave from the OSG, and make the reflected shock pass over the NSH, it would have to be placed very low in the tunnel and would nearly be immersed in the bottom boundary layer.

4. Effect of Wedge Angle (Mach 2.00, 8.5° OSG, 50% wedge design length)

The final configuration presented is shown in Figure 22, which uses the M 2.00 nozzle with an 8.5° angle OSG. This configuration will produce a Mach number of 1.4 in front of the normal shock (had the NSH been included). This case started but again has considerably nonuniform flow in the region before the normal shock because of the interaction of the reflected shock and the OSG expansion wave.

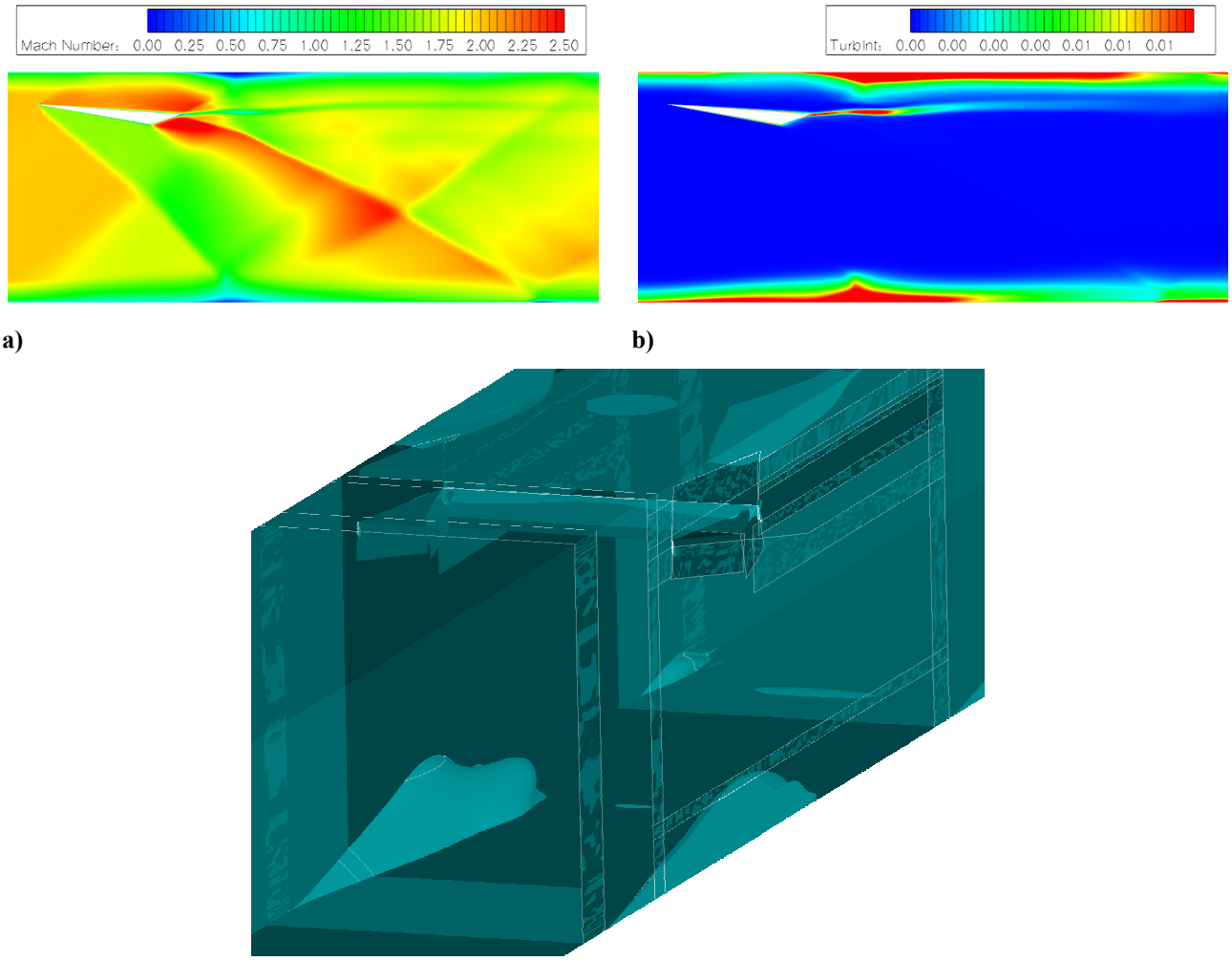

Figure 21. Mach 2.75, 10° OSG, 50% wedge design length. a) Tunnel centerline colored by Mach contours from 0.0 – 2.5, b) Tunnel centerline colored by turbulent intensity contours from 0 – 1% c) Tunnel with iso surfaces of separated regions.

F. Unsteady Start from Quiescent Flow

It was observed that the existing nozzles are asymmetric top/bottom. The flow along the top curved wall accelerates more than along the bottom wall producing thinner boundary layers along the top wall than along the bottom wall. This is beneficial for the current investigation since the bottom boundary layer needs to develop to a certain thickness in a short distance. However, the steady state simulations ignore the start up transients.

For this reason UC computed several simulations from quiescent initial conditions with an instantly applied low backpressure. The results showed that a large separation bubble is produced on the bottom wall and a smaller one on the top wall once the flow is sufficiently accelerated. These bubbles travel downstream and for some cases are purged from the tunnel. The results suggest that these separation bubbles can cause transient startup problems due to the additional blockage they produce. These results should be considered preliminary since they do not time accurately model the exit pressure drop, but they do suggest that if these separation bubble cause too many problems a symmetric nozzle may be needed.

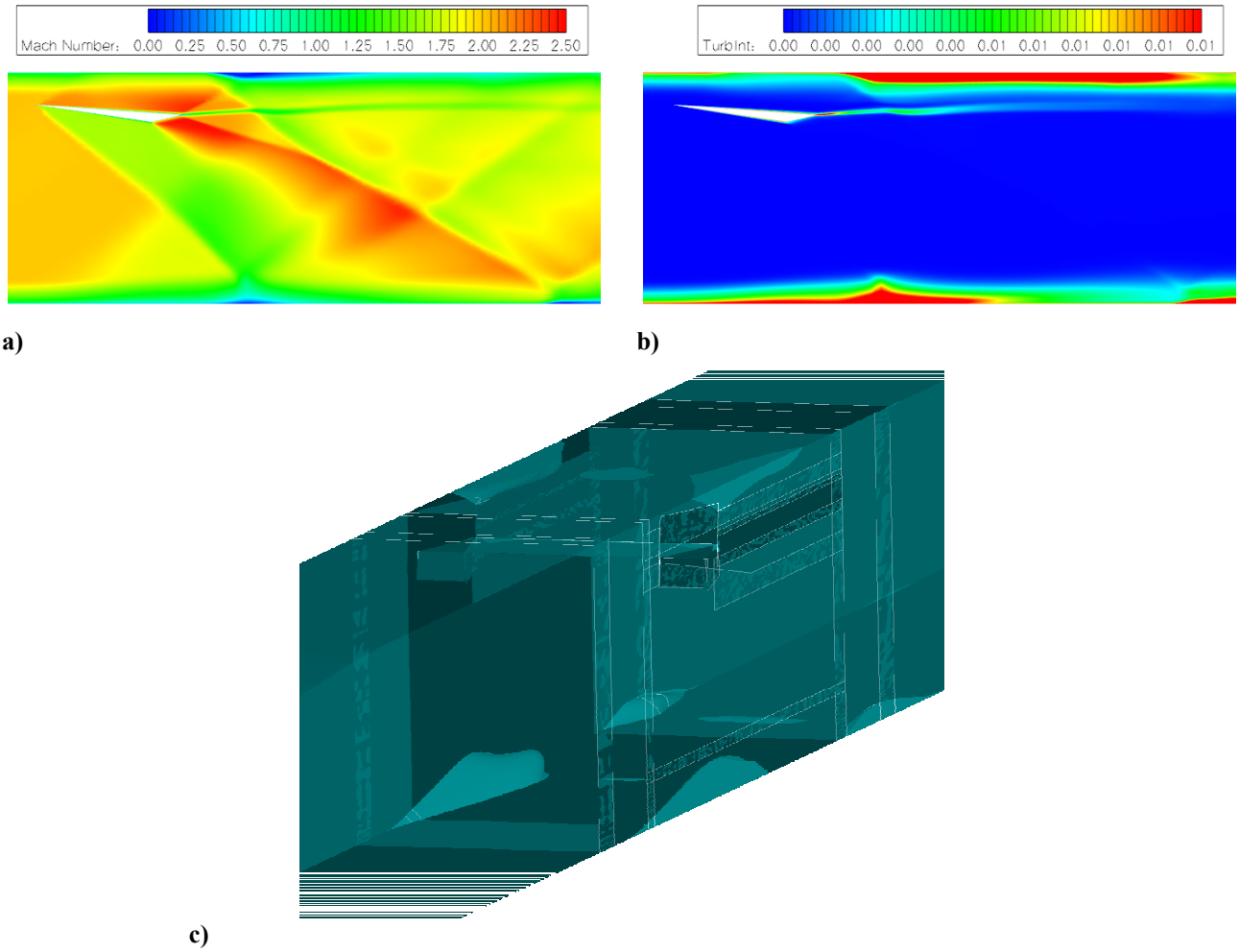

Figure 22. Mach 2.00, 8.5° OSG, 50% wedge design length. a) Tunnel centerline colored by Mach contours from 0.0 – 2.5, b) Tunnel centerline colored by turbulent intensity contours from 0 – 1% c) Tunnel with iso surfaces of separated regions.

VII. Conclusions and Future Work

The design of a new supersonic inlet test configuration has been explored in CFD while some configurations have simultaneously been run experimentally. This combined CFD and experimental approach will lead to better understanding, and a more robust final design. Design goals have been established, and the design space has been explored considering a new tunnel as well as using an existing tunnel at the University of Michigan. The design has been parameterized, and a meshing procedure has been set up so the mesh can easily be modified for different wedge and tunnel geometries. Preliminary simulations have been completed that verify the design procedure, and give insight into the behavior of the flowfield in the tunnel. However, in order to start the existing Mach 2.00 and Mach 2.75 configurations, the geometry had to be modified until there was little room left in the flowfield to insert the NSH. Some of the design constraints could be relaxed in order to start and run the tunnel, but it would compromise some of the design goals. It is also possible to use the existing tunnels to help further explore some of the design parameters experimentally. However, in order to meet all the design objectives, it is recommended that a new tunnel be designed with an inflow design Mach number of 1.8. This tunnel would resemble the configuration described in the design procedure section, but it would be optimized to produce a more desirable amount of blockage and would also allow for a sufficient runtime to conduct the experiment. This tunnel would most likely be taller to give more room between the oblique shock reflection and the normal shock. It would also be wider to produce a cleaner SBLI as seen in the double wide configuration.

Acknowledgments

This work was supported by the U.S. Air Force Collaborative Center for Aeronautical Sciences. The authors would like to thank the Air Force Research Laboratory, Air Vehicle Directorate, AFRL/RB and Drs. John Benek, Jon Tinapple, and Lewis Suber for their guidance and support.

References

[1]Pitt Ford, C. W., Babinsky, H., "Micro-Ramp Control for Oblique Shock Wave/Boundary Layer Interactions," AIAA 2007-4115, June 2007.

[2]Doerffer, P., Hirsch, C., Dussauge, J-P., Babinsky, H., Barakos, G.N. (Eds), Unsteady Effects of Shock Wave induced Separation: (Notes on Numerical Fluid Mechanics and Multidisciplinary Design), Springer.

[3]Lapsa, A.P., "Experimental Study of Passive Ramps for Control of Shock–Boundary Layer Interactions," Ph. D. Dissertation, Aerospace Engineering Dept., University of Michigan, Ann Arbor, MI, 2009.

[4]Seddon J., Goldsmith E.L., Intake Aerodynamics, Blackwell 2nd Ed. 1999.

[5] DeBonis, James R., Oberkampf, William L., Wolf, Richard T., Orkwis, Paul D., Turner, Mark G., and Babinsky, Holger, "Assessment of CFD Models for Shock Boundary-Layer Interaction," AIAA-2010-4823, Chicago, IL, June, 2010.

[6]Settles, G. S., Frank K. Lu, F. K., "Conical Similarity of Shock/Boundary-Layer Interactions Generated by Swept and Unswept Fins," AIAA journal, Vol. 23, No. 7, July 1985.

[7]Nagel, Z. and Dahm, W.J.A. "Direct assessment of spatial resolution in particle-image velocimetry measurements," University of Michigan, MI, 2008

[8]MATLAB, R2008a, The MathWorks, Inc., MA 2010.

[9]P.G. Buning, D.C. Jespersen, T.H. Pulliam, W.M. Chan, J.P. Slotnick, S.E. Krist, K.J. Renze, Overflow User's Manual, Version 1.8g, NASA Langley Research Center, Hampton, VA, 1999.

[10]Benek, J. A., Steger, J. L., and Dougherty, F. C. "A Flexible Grid Embedding Technique with Application to the Euler Equations." AIAA Paper 83-1944, 1983.

[11]Toro, E. F., Spruce, M., and Speares, W., "Restoration of the Contact Surface in the HLL Riemann Solver," Shock Waves, Vol. 4, 1994 pp 25-34.

[12]Koren, B., "Upwind Schemes, Multigrid and Defect Correction for the Steady Navier-Stokes Equations," Proceedings of the 11th International Conference in Numerical Methods in Fluid Dynamics, edited by D. L Dwoyer, M. Y. Hussani, and R. G. Voigt, Springer-Verlag, Berlin 1989.

[13]Tramel, R. W. and Nichols, R. H., "A Highly Efficient Numerical Method for Overset-Mesh Moving–Body Problems," AIAA-97-2040, June 1997.

[14]Pointwise, Ver. 16.03, Pointwise, Inc., Fort Worth, TX, 2010.